

## 17 Methods used and highlighted results from UMIST

J. Uribe, S. Utyuzhnikov, A. J. Revell, A. Gerasimov,  
and D. Laurence, UMIST (The University of Manchester)

### Abstract

The preferred models of the consortium (SSG, k-w, STT, SCW) have been implemented in a recent open source FV software and tested. Numerical behaviour of two popular versions of the V2F model have been compared and a new formulation proposed, that combines the accuracy of the original version and stability of the degraded “code friendly version”. In the DES framework, the need for reduction of the EVM coefficient has been related to the stress-strain misalignment in rapidly changing time dependent mode and a single transport equation for this coefficient proposed. On the wall function front, the AWF of Craft and Gerasimov entailing an analytical integration of terms over the first cell (body force in particular) proved challenging to implement on unstructured grids, but was achieved. Towards the end of the project, a promising mathematical framework (Robin type conditions) was proposed, based on domain decomposition and mixed Dirichlet and Neumann conditions.

### 17.1 Introduction

The focus at UMIST has been set on “robust” formulations of the models and wall treatment, for implementation in professional software, and their suitability for industrial applications. Collaborations with Ansys-CFX and NUMECA, in addition to EDF, have been very fruitful in this respect. After fine tuning of the turbulence models in academic codes, UMIST implemented these models in the EDF unstructured finite volume software of EDF named *Code\_Saturne*, described in Chapter II.9 (this software is available in full source code to academic partner-developers contributing to the *Code\_Saturne* consortium). One exception is test-case 1 (wing-tip vortex) performed by C. Robinson with UMIST’s STREAM code, but this as part of the MDAW project, and hence not described herein although those solutions will appear in chapter IV.

### 17.2 Two equations models improvements

#### 17.2.1 Near-wall models

The viscous effects are not taken into account when using a wall function approach, therefore losing information that can be important in some flows. In order to reproduce the near-wall effects, a low-Reynolds model should be used to compute all the sharp gradients present in the viscous sublayer. Many two equation models have a low-Reynolds counterpart but they have been developed (as if an afterthought) via damping functions in order to obtain the correct behaviour near the wall. These damping functions are usually designed for a specific

type of flow and are far from universal. Most of them contain the distance from the wall as a parameter, which can be ill-defined in certain geometries.

Durbin (1991) proposed a more physical approach to the near wall modelling by taking into account the effects of the wall via an elliptic equation. The formulation of the V2F model is based on the use of the correct velocity scale near the wall,  $\overline{v^2}$  instead of  $k$ . Using this rationale, the turbulent viscosity is computed as  $\nu_t = C_\mu \overline{v^2} T$ , where  $T$  is a maximum between the turbulent and the Kolmogorov timescales. Additionally to the  $k$  and  $\varepsilon$  equations, a transport equation is solved for  $\overline{v^2}$  and an elliptic equation is solved for  $f$ . The V2F model was proven to reproduce the wall effects accurately in many types of flows (Kalitzin 1999) but its major drawback is the stiffness present at the wall due to the boundary condition of the elliptic function  $f$ . At the wall, the boundary condition is given by:

$$f_w = \lim_{y \rightarrow 0} \frac{-20\nu \overline{v^2}}{\varepsilon_w y^4}$$

The fact that the denominator includes the distance to the wall to the power of four makes it very stiff and a coupled algorithm is necessary to obtain convergence (Lien and Kalitzin, 2001). It also imposes constraints on the mesh size near the wall.

During the course of the FLOMANIA project, UMIST developed a new formulation of the model that removes the stiffness while retaining the advantages of the original formulation (Laurence et al 2004). The new model solves for a variable  $\overline{\varphi} = \overline{v^2}/k$ , and by adding a change on the definition of  $f$ ,  $\overline{f} = f + \frac{2\nu}{k} \frac{\partial k}{\partial x_k} \frac{\partial \overline{\varphi}}{\partial x_k} + \nu \frac{\partial^2 \overline{\varphi}}{\partial x_k^2}$ . the equations can be solved uncoupled. The final equations for the two variables are:

$$\begin{aligned} \frac{D\overline{\varphi}}{Dt} &= \overline{f} - P \frac{\overline{\varphi}}{k} + \frac{2}{k} \frac{\nu_t}{\sigma_k} \frac{\partial \overline{\varphi}}{\partial x_j} \frac{\partial k}{\partial x_j} + \frac{\partial}{\partial x_j} \left[ \frac{\nu_t}{\sigma_k} \frac{\partial \overline{\varphi}}{\partial x_j} \right] \\ L^2 \nabla^2 \overline{f} - \overline{f} &= \frac{1}{T} (C_1 - 1) \left[ \overline{\varphi} - \frac{2}{3} \right] - C_2 \frac{P}{k} - 2 \frac{\nu}{k} \frac{\partial \overline{\varphi}}{\partial x_j} \frac{\partial k}{\partial x_j} - \nu \nabla^2 \overline{\varphi} \end{aligned}$$

with the now simple, uncoupled, boundary conditions  $f = 0$  and  $\overline{\varphi} = 0$ .

It is shown that the cross terms (products of gradients) are comparatively small and do not cause any stability problems.

The model was implemented in the unstructured FV *Code\_Saturne*. The new formulation proposed presents an overall good performance, similar to the original model which required very small time steps (i.e. CFL of order 0.01, probably as a consequence of not being able to couple the boundary conditions in the professional FV code), whereas the above version convergence much more easily (CFL of order 1).

The  $\overline{\varphi}$  model was tested on the asymmetric plane diffuser with other elliptic relaxation formulations as described (Laurence et al 2004). The velocity profiles predicted by the  $\overline{\varphi}$  model, the LDM [V2F\_Li] and the  $k-\omega$  (dashed, solid and dotted lines, accordingly) are shown in Figure 2. The computational results are

compared against the experimental data marked by triangles. The LDM underpredicts the recirculation length whereas the  $\phi$ -model gives a larger recirculation zone, closer to the experiment. Overall, the  $\phi$ -model performs better than the LDM. It should be noted that the pressure field is very sensitive to the recirculation bubble and affects the bulk of the flow as can be seen concerning the mean velocity in the region of the straight wall. The LDM model underestimates the velocity in this region, similarly to more standard  $k - \epsilon$  models.

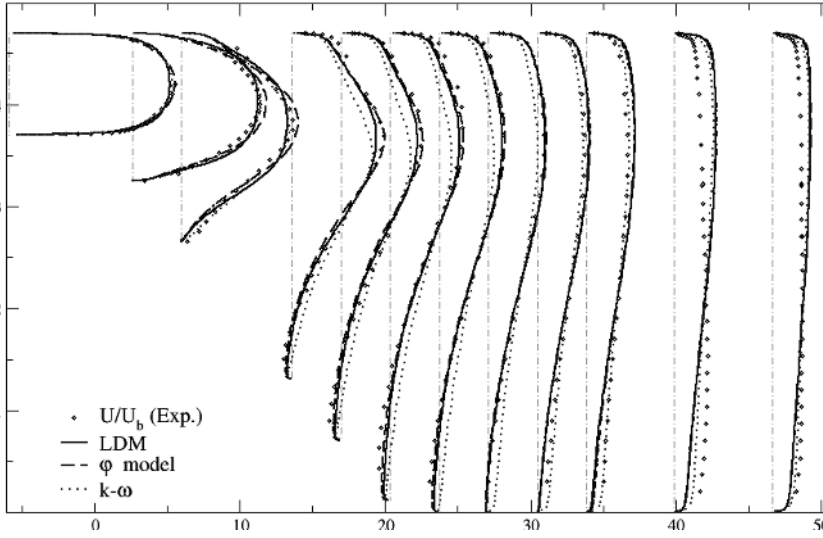


**Figure 2** Asymmetric plane diffuser. Velocity profiles

The pressure coefficients are shown in Fig. 3. Here again, the  $\phi$ -model produces better prediction than the LDM; while the both models are more accurate than the  $k - \omega$ .

**Flow over periodic hills.**

Velocity profiles for the flow over periodic hills can be seen in figure 4. Here the  $\phi$  model performs better than the standard  $k - \epsilon$ .

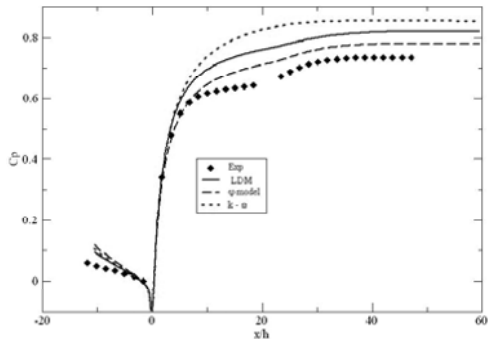


**Figure 3** Pressure coefficient

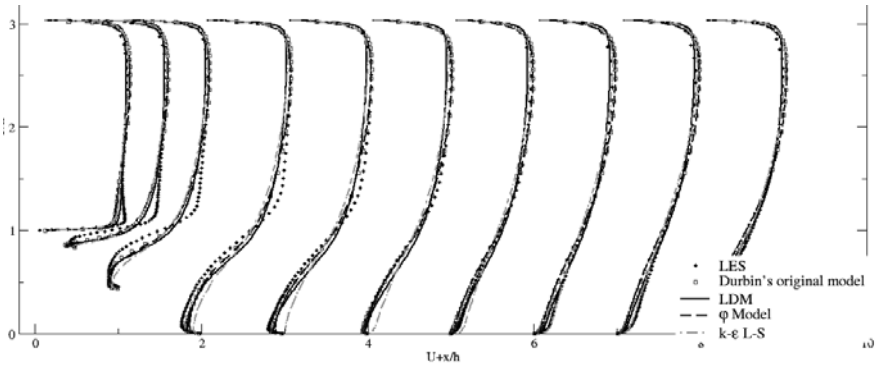


**Figure 4** Flow over periodic hills. Velocity profile

17.2.2 *New stress-strain eddy viscosity model:  $k - \epsilon - C_{as}$*

A new eddy viscosity model was developed to include stress-strain lag effects in the modelling of unsteady mean flows. Standard EVMs significantly over-predict the production of turbulent kinetic energy in presence of strong strain. This has led to various limiters as in the V2F model (Durbin 1995), the SSTmodel (Menter et al. 2003) and the Linear Production model (Guimet et al 2002) among others. These corrections are not needed in DSMs, and Jakirlić (2004) solves in fact the full RSM to include stresses only in the  $k$  production term as a means of improving levels of  $k$ , while the standard EVM representation of the stresses is subsequently applied to the momentum equation. The results show some good improvements, but the computational cost is very high. The aim of this work was therefore to develop a model for the stress-strain lag, which appears to be a key parameter in rapidly evolving flows. The stress-strain lag parameter, hereby denoted  $C_{as}$  is written as follows.

$$C_{as} = -\frac{a_{ij}S_{ij}}{\|S\|} \quad \|S\| = \sqrt{2S_{ij}S_{ij}}$$

A transport equation for  $C_{as}$  is derived from the full SSG DSM for the time derivative of the anisotropy tensor,  $a_{ij}$ , as well as terms including the rate of change of the strain tensor,  $S_{ij}$  (Revell et al). The stress-strain lag term is defined as follows. The strain rate parameter is  $\eta = k\|S\|/\epsilon$ , and the second invariant of anisotropy is  $A_2 = a_{ij}a_{ij}$ . The final transport equation is therefore as follows.

$$\begin{aligned} \frac{DC_{as}}{Dt} = & \left(0.266 + 0.325\sqrt{A_2}\right)\|S\| - 2.7\frac{\epsilon}{k}C_{as} + 0.1\|S\|C_{as}^2 + 1.05\frac{S_{ij}a_{ik}a_{kj}}{\eta} \\ & + 0.75\frac{S_{ij}a_{ik}S_{jk}}{\|S\|} + 1.6\frac{S_{ij}a_{ik}\Omega_{jk}}{\|S\|} - \frac{a_{ij}}{\|S\|}\frac{DS_{ij}}{Dt} - \frac{C_{as}}{\|S\|}\frac{D\|S\|}{Dt} + \text{Diff}^{C_{as}} \end{aligned}$$

The turbulent viscosity,  $\nu_t$ , is redefined using an updated value of  $C_\mu$  according to the following limit. The new diffusion term is of a standard gradient diffusion form with the constant  $\sigma_{C_{as}}=2$ .

$$\nu_t = C_\mu^{new} \frac{k^2}{\varepsilon} \quad C_\mu^{new} = \min\left(0.09, \frac{C_{as}}{\eta}\right)$$

If the equation is to correctly model the log-layer region, then it is a requirement that it returns the standard value of  $C_\mu$  in equilibrium conditions (i.e. when production to dissipation ratio is unity and  $h=3.33$ ). The correctional effects of the  $C_{as}$  term on the parameter  $C_\mu$  are expected to be even greater since normal anisotropy is non-zero and so more of the terms in the transport equation are in play. The motivation behind the model development stems from the observation that in rapidly varying mean flows, such as bluff body wakes or staggered tube bundles, RSMs can produce large unsteady structures similar to LES (Benhamadouche et al 2003). In homogenous turbulence subject to cyclic straining it was shown that the stresses increasingly lag behind the strains until production is shut off (Hadzic et al 2001). Therefore RSMs seem an attractive idea for DES, but are too computationally expensive. The present model is very economical since it has almost no additional expense over a standard 2 equation model in terms of convergence time, and only slightly higher storage requirements. It is also very easy to implement in contrast with the RSM.

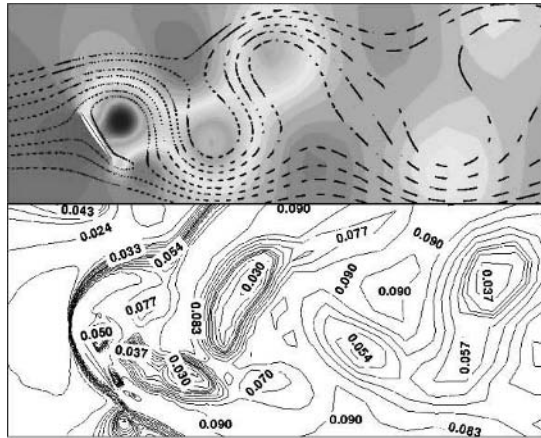


**Figure 1.** Flow around NACA0012 at  $60^\circ$  incidence using  $k-\varepsilon-C_{as}$  model. *top:* Pressure contours & streamlines. *Bottom:* modified  $C_\mu$  isovalues

Figure 1 shows contour plots from some early calculations on the NACA0012 airfoil at an AoA of  $60^\circ$ . This is a massively separated flow and it can be seen that  $C_\mu$  is reduced in the regions corresponding to the shedded structures (shown by the pressure contours and flow streamlines) while recovering its usual values at the boundaries of the unsteady wake. This behaviour is in agreement with the

prediction of strongly detached flows by modified two-equation models that suggest the  $C_\mu$  reduction based on the behaviour of the RSM modelling for the same class of flows (Hoarau et al 2002), in the context of Organised Eddy Simulation. It appears that the response of the model to regions of stress-strain lag could be used to automatically reduce  $k$  levels in the URANS-DES transition when unsteady structures start to emerge, instead of the ad-hoc switch based on grid characteristics as commonly used in DES; in which mesh dependency is one of the current breakdowns.

### 17.2.3 Generalized (Robin-type) wall functions

A method of boundary conditions transfer has been developed (Utyuzhnikov 2005). The method allows one to transfer a boundary condition from a wall to some intermediate surface. The boundary condition on the intermediate surface always becomes of Robin-type. In the vicinity of the wall, the boundary condition can be treated as the generalized wall function. Meanwhile, one should note the method can also be used far from the wall in the framework of a domain decomposition method.

If a Dirichlet boundary condition is set for a function  $u$  on the wall, the wall function (boundary condition) is formulated at point  $y^*$  (in the normal to the wall direction) as follows (Utyuzhnikov 2005)

$$u(y^*) = u_0 + y^* \frac{du}{dy}(y^*) f_1 - \frac{y^{*2}}{2\mu^*} \left( \int_0^1 R_h d\xi \right) f_2,$$

where  $f_1 = \int_0^1 \frac{\mu(y^*)}{\mu(\xi)} d\xi$ ,  $f_2 = 2 \int_0^1 \mu(y^*) / \mu(\xi) \left( 1 - \int_0^\xi R_h d\xi' / \int_0^1 R_h d\xi \right) d\xi$ ,  $u(0) = u_0$ ,  $R_h = R_h(y)$  is the right-hand side of the governing equation written in the boundary-layer-like form [1-3].

If the coefficient  $\mu$  is changed piece-wise linearly [3] and  $R_h = const$ ,

$$\mu = \begin{cases} \mu_w & \text{if } 0 \leq y \leq y_v \\ \frac{y - y_v}{y^* - y_v} (\mu^* - \mu_w) + \mu_w & \text{if } y_v \leq y \leq y^* \end{cases}$$

then it is possible to obtain analytical expressions for  $f_1$  and  $f_2$ :

$$f_1 = \alpha_\mu \bar{y}_v (1 + \theta \ln \alpha_\mu), \quad f_2 = 2\alpha_\mu \bar{y}_v \left[ 1 - \theta - (1/2 - \theta) \bar{y}_v + \alpha_\mu \bar{y}_v \theta^2 \ln \alpha_\mu \right],$$

$$\text{where } \bar{y}_v = y_v / y^*, \alpha_\mu = \mu^* / \mu_w, \theta^{-1} = \frac{\mu^* - \mu_w}{\mu_w} \frac{y_v}{y^* - y_v}.$$

The obtained general form of the wall function has been implemented for all independent variables (except dissipation  $\varepsilon$ ) including the turbulent kinetic energy  $k$  and normal component of the velocity. These wall functions are formulated in the differential form, they are robust and can be applied to any kind of approximations of the governing equations. Boundary conditions are transferred to the point  $y^*$  which can be completely mesh independent.